

## Can the QCD running coupling have a causal analyticity structure?

Einan Gardi <sup>a</sup>, Georges Grunberg <sup>b</sup> and Marek Karliner <sup>a</sup>

<sup>a</sup> School of Physics and Astronomy  
Raymond and Beverly Sackler Faculty of Exact Sciences  
Tel-Aviv University, 69978 Tel-Aviv, Israel  
e-mail: gardi@post.tau.ac.il, marek@proton.tau.ac.il

<sup>b</sup> Centre de Physique Théorique de l'Ecole Polytechnique \*  
91128 Palaiseau Cedex, France  
email: grunberg@cpht.polytechnique.fr

### Abstract

Solving the QCD renormalization group equation at the 2-loop and 3-loop orders we obtain explicit expressions for the coupling as a function of the scale in terms of the Lambert W function. We study the nature of the “Landau singularities” in the complex  $Q^2$  plane and show that perturbative freezing can lead, in certain cases, to an analyticity structure that is consistent with causality. We analyze the Analytic Perturbation Theory (APT) approach which is intended to remove the “Landau singularities”, and show that at 2-loops it is uniquely defined in terms of the Lambert W function, and that, depending on the value of the first two  $\beta$  function coefficients  $\beta_0$  and  $\beta_1$ , it is either consistent with perturbative freezing (for  $\beta_1 < -\beta_0^2$ ) with an infrared limit of  $-\beta_0/\beta_1$  or leads to a non-perturbative infrared coupling with a limit of  $1/\beta_0$  (for  $\beta_1 > -\beta_0^2$ ). The possibility of a causal perturbative coupling is in accordance with the idea that a purely perturbative Banks-Zaks phase with an infrared fixed-point exists in QCD if the number of flavours ( $N_f$ ) is increased. The causality condition implies that the perturbative phase is realized for  $N_f \geq 10$ .

---

\*CNRS UMR C7644

# 1 Introduction

Due to asymptotic freedom [1], physical quantities in QCD at large momentum transfers  $Q^2 \equiv -q^2$ , where  $q^2$  is a space-like momentum-squared, can be calculated as power expansions in the coupling constant  $x(Q^2) = \alpha_s(Q^2)/\pi$ . This seems as a reasonable expansion<sup>†</sup> since the coupling vanishes at this limit according to:

$$x(Q^2) \sim \frac{1}{\beta_0 \ln(Q^2/\Lambda^2)} \quad (1)$$

where

$$\beta_0 = \frac{1}{4} \left( 11 - \frac{2}{3} N_f \right) \quad (2)$$

and  $\Lambda$  is the QCD scale.  $x(Q^2)$  in (1) is a solution to the 1-loop renormalization group (RG) equation

$$Q^2 \frac{dx}{dQ^2} = -\beta_0 x^2. \quad (3)$$

Going to lower  $Q^2$ ,  $x(Q^2)$  becomes larger, and higher loops have to be taken into account in (3), as well as in the expansions that describe physical quantities in terms of  $x(Q^2)$ . The RG equation at the  $(n+1)$ -th loop order is

$$Q^2 \frac{dx}{dQ^2} = \beta(x) = -\beta_0 x^2 (1 + c_1 x + c_2 x^2 + \dots + c_n x^n). \quad (4)$$

For  $Q^2$  below  $\Lambda^2$ , non-perturbative effects, which are non-expandable in  $x(Q^2)$ , become dominant, and the perturbative expansion becomes useless. However, in the intermediate regime, the perturbative solution can be fitted to the data, provided it is supplemented by power-like terms. These terms are non-perturbative but they can be characterized by perturbation theory, as they are related to the large order asymptotics of the perturbation series, and in particular to renormalons (see [2] and refs. therein). It is the non-convergence of the perturbative expansion, that provides some information on the non-perturbative terms.

Another indication that the perturbative result is incomplete, and cannot describe the low  $Q^2$  physics unless it is supplemented by non-perturbative corrections, comes from considering its analyticity structure in the complex  $Q^2$  plane: a generic QCD observable, that depends on a space-like momentum variable  $Q^2$ , is expected to be an analytic function of  $Q^2$  in the entire complex plane, except the negative real (time-like) axis. Singularities on the time-like axis are meaningful since they correspond to production of on-shell particles, while existence of singularities away from the time-like axis would violate causality. Thus causality constrains the functional dependence of observables on  $Q^2$ . The analyticity condition is equivalent to the requirement that  $x(Q^2)$  obeys the following dispersion relation:

$$\beta_R(s) \equiv -\frac{1}{\pi} \text{Im}\{x(-s)\} \quad (5)$$

---

<sup>†</sup>Even though the series actually does not converge, and in-fact it is non Borel-summable.

with

$$x(Q^2) = - \int_0^\infty ds \frac{\beta_R(s)}{s + Q^2} \quad (6)$$

where  $\beta_R(s)$ , with  $0 \leq s < \infty$ , is called the spectral density function.

A 1-loop perturbative result for a generic QCD observable depends on the coupling (1) and therefore contains a “Landau-pole” at  $Q^2 = \Lambda^2$ . This pole is located on the positive real axis (the space-like axis) and therefore it is non-physical. This pole is expected to be washed out when further perturbative and non-perturbative corrections are added. In general, higher loop perturbative results for the coupling have a more complicated analyticity structure which is still inconsistent with causality. Thus, in general, causality can be saved only by inclusion of non-perturbative terms.

A special case in which the perturbative result by itself can be consistent with causality, is when the perturbative  $\beta$  function (4) has a zero. Then, the coupling reaches a finite value in the infrared limit and thus it is finite for any real and positive  $Q^2$ . To be consistent with causality, the coupling should be non-singular in the entire  $Q^2$  plane except the time-like axis, and therefore there may be cases where freezing occurs but causality is still violated, due to complex  $Q^2$  singularities.

In real-world QCD, with only three light flavors, it seems from the first few terms in the  $\beta$  function series that there is no perturbative freezing [3]. In this case, the standard perturbative approach always faces the “Landau singularity” problem. Refs. [4, 5] revive a natural solution to this problem through the so-called Analytic Perturbation Theory (APT) approach. The APT coupling was used in [7] for discussing power corrections within the more general (non-perturbative) dispersive approach of [6], and was also considered there (as well as in refs. [2, 8]) as a possible model for non-OPE power terms.

In this paper we solve the 2-loop and 3-loop RG equation giving explicit expressions for the coupling as a function of the scale in terms of the Lambert W function. This enables us to study the location and the nature of the “Landau singularities” in the complex  $Q^2$  plane. In particular we find exact criteria which determine when perturbative freezing à la Banks-Zaks [10] leads to an analyticity structure that is consistent with causality. Using the Lambert W solution, we then analyze the APT approach and show that it is either consistent with perturbative freezing (for  $c < -\beta_0 < 0$ ) with an infrared limit of  $-1/c$ , or leads to a non-perturbative coupling with an infrared limit of  $1/\beta_0$  (for  $c > -\beta_0$ ).

## 2 The Lambert W function – exact explicit coupling at 2-loops

We start with a 2-loop RG equation

$$\beta(x) = \frac{dx}{dt} = -\beta_0 x^2 (1 + cx) \quad (7)$$

where  $t = \ln(Q^2/\Lambda^2)$ . Note that the value of  $\Lambda$  here should be different from the one in (1), so that the same phenomenological value for  $x(Q^2)$  will be obtained. When higher-order corrections are added,  $\Lambda$  should be further adjusted, but for simplicity we use the same notation throughout. The 2-loop coefficient  $c$ , which is renormalization scheme independent, is given by:

$$c = \frac{\beta_1}{\beta_0} = \frac{1}{4\beta_0} \left[ 102 - \frac{38}{3} N_f \right] \quad (8)$$

A straightforward integration of (7) for the asymptotically-free case ( $\beta_0 > 0$ ) yields:

$$\beta_0 \ln(Q^2/\Lambda^2) = \frac{1}{x} - c \ln \left[ \frac{1}{x} + c \right] \quad (9)$$

At this stage it is already clear that  $x(Q^2)$  has a cut on the negative real axis, being a function of  $\ln(Q^2/\Lambda^2)$ . The problem of inverting (9) makes it difficult to study the singularity structure. In [4], for instance, the inversion of (9) relies on the assumption that the  $1/x$  term is much larger than the logarithmic term. Although correct in the deep perturbative region, this approximation is inadequate for studying the singularity structure of  $x(Q^2)$ . In particular, this approximation does not allow perturbative freezing at all, since in the latter case the logarithmic term becomes dominant in the infrared region.

Luckily, an explicit solution of the 2-loop RG equation (7), i.e. an inversion of (9), can be written in terms of the so-called Lambert  $W$  function [11].  $W(z)$  is defined by

$$W(z) \exp [W(z)] = z \quad (10)$$

The coupling is then given by:

$$x(Q^2) = -\frac{1}{c} \frac{1}{1 + W(z)} \quad (11)$$

$$z = -\frac{1}{c} \exp(-1 - \beta_0 t/c) = -\frac{1}{c e} \left( \frac{Q^2}{\Lambda^2} \right)^{-\beta_0/c}$$

$W(z)$  is a multi-valued function with an infinite number of branches, denoted by  $W_n(z)$ . We follow [11] as for the division of the branches and notation. The requirement that  $x(Q^2)$  is real and positive for a real positive  $Q^2$  (at least for  $Q^2 \gg \Lambda^2$ ), is sufficient to determine the physical branch depending on the sign of  $c$ :

- (a) for  $c > 0$ ,  $z < 0$  and the physical branch is  $W_{-1}(z)$ . This branch is a real monotonically decreasing function for  $z \in (-1/e, 0)$ , with  $W_{-1}(z) \in (-\infty, -1)$  (outside this range  $W_{-1}(z)$  is complex). Thus, the ultraviolet limit corresponds to  $z \rightarrow 0^-$ ,  $W_{-1}(z) \rightarrow -\infty$ , and  $x \rightarrow 0^+$ , as required by asymptotic freedom. In the infrared region, below the ‘‘Landau singularity’’ (see further discussion later)  $x$  is complex.

- (b) for  $c < 0$ ,  $z > 0$  and the physical branch is the principal branch,  $W_0(z)$ . This branch is a real monotonically increasing function for  $z \in (-1/e, \infty)$ , with  $W_0 \in (-1, \infty)$  (outside this range,  $W_0(z)$  is complex). For  $z \geq 0$ ,  $W_0(z) \in [0, \infty)$ . The ultraviolet limit corresponds to  $z \rightarrow \infty$ ,  $W_0(z) \rightarrow \infty$  and  $x \rightarrow 0^+$ . The infrared limit corresponds to  $z \rightarrow 0^+$ ,  $W_0(z) \rightarrow 0^+$ , and  $x \rightarrow (-1/c)^-$  which is consistent with the Banks-Zaks perturbative fixed-point value  $x_{FP} = -1/c$ .

The solution in (11) can be quite useful whenever a two-loop evolution of the QCD coupling is required. It clearly yields more accurate results than the standard expansion of the coupling in  $1/\ln(Q^2/\Lambda^2)$ . Note that the latter can be obtained from (11) using the asymptotic formulae for  $W(z)$ : for  $c < 0$  one uses the asymptotic expansion of  $W_0(z)$  at large positive  $z$  that starts with  $W_0(z) \sim \ln(z) - \ln(\ln(z))$ , and for  $c > 0$  one uses the asymptotic expansion of  $W_{-1}(z)$  at small negative  $z$  that starts with  $W_{-1}(z) \sim \ln(-z) - \ln(-\ln(-z))$ .

Other possible applications of (11) are in the context of resummation methods, such as the iterated construction suggested by Maxwell in [12] and the improved Baker-Gammel approximants suggested by Cvetič in [13] which both generalize the diagonal Padé approximants approach [14].

The general idea in these resummation methods is that knowledge of the first few orders in a perturbative expansion, together with the RG equation, can be used to construct approximants to physical quantities that have a better accuracy than the truncated perturbative series, and exhibit reduced renormalization scale and scheme dependence (for related ideas, see [15, 16]). Diagonal Padé Approximants, as opposed to truncated series, are exactly invariant with respect to an arbitrary renormalization scale transformation, so long as the transformation respects the 1-loop evolution form (i.e. an evolution related to the 1-loop  $\beta$  function) [14]. In order to achieve scale invariance beyond this approximation, it turns out [12, 13] that one has to use more complicated functions, which are related to the inverted solution of the some higher-order RG equation. Using the explicit inverted solution of the 2-loop RG equation (11) the methods of [12, 13] can be easily implemented in practice and also their mathematical structure can be further studied.

It is worth mentioning that another way<sup>‡</sup> to invert (9) was suggested in the past by Khuri and Ren [17]: they wrote the 2-loop coupling in terms of  $F(\zeta)$ , which is defined by  $2F(\zeta) - \exp[F(\zeta)] + 1 = \zeta$ . The latter equation was considered earlier in different physical contexts (see refs. in [17]). There is, of course, a one-to-one correspondence between the Lambert W solution of (11) and that of [17]:

$$-\frac{1}{2} \exp [F(\zeta)] = W \left( -\frac{1}{2} \exp \left[ \frac{1}{2}(\zeta - 1) \right] \right). \quad (12)$$

In the following we stick with the Lambert W solution.

---

<sup>‡</sup>An exact solution of (9) in term of a (modified) Borel representation can also be found in [18].

### 3 The singularity structure of the 2-loop coupling

Having found an explicit solution for coupling (11), we would like now to analyze its singularity structure in the complex  $Q^2$  plane and, in particular, to find when it is consistent with causality. To do so it is essential to define the analytical continuation of  $x(Q^2)$  to the whole complex  $Q^2$  plane, namely to specify the branch of  $W(z)$  that is used in (11) for a generic  $Q^2 = |Q^2|e^{i\phi}$ , where  $-\pi < \phi < \pi$ .

At this stage it is necessary to give a brief description of the singularity structure of the Lambert  $W$  function; more details can be found in [11]. The partition of the complex  $W$  plane between the different branches,  $W_0$ ,  $W_{\pm 1}$  and  $W_{\pm 2}$ , is shown by dashed lines in fig. 1 (the other lines in fig. 1 will be discussed later). It is important to realize that the singularity structure of the different branches  $W_n(z)$  is different.  $W_0$ ,  $W_{-1}$  and  $W_1$  share a common branch point at  $z = -1/e$ , at which  $W = -1$ . The  $z = -1/e$  cut in all three branches is chosen to be  $z \in (-\infty, -1/e)$ . While for  $W_0$ ,  $z = -1/e$  is the only singularity, other branches  $W_n(z)$  with  $n \neq 0$  have a branch point at  $z = 0$  with a cut at  $(-\infty, 0)$ . The  $z = 0$  cut is the only singularity in  $W_n$  for  $n \geq 2$ . Note that  $W(y)$  obeys the following symmetry [11],

$$W_{-n}^*(y^*) = W_n(y) \quad (13)$$

and therefore it is possible to obtain  $W(z)$  and  $x(Q^2)$  on the upper half-plane from those on the lower half-plane. Note also that the branches  $W_{-1}(z)$  and  $W_1(z)$  have a common real limit along the cut for  $z \in (-1/e, 0)$ . It is only a matter of convention that the negative real axis ( $W \in (-\infty, -1/e)$ ) belongs to  $W_{-1}$  rather than to  $W_1$ .

The criterion we use for defining the analytical continuation is that for  $|Q^2| \gg \Lambda^2$ , the coupling  $x(Q^2)$ , and therefore also  $W(z)$ , will be continuous as a function of the phase of  $Q^2$ . From the analyticity structure of  $W(z)$  described above it is clear that as long as the phase of  $z$  does not reach  $\pm\pi$  for any  $Q^2$  in the first sheet, the only relevant branch is the physical one, i.e. the one that yields a real positive  $x$  for real positive  $Q^2$ :  $W_0$  for  $c < 0$  and  $W_{\pm 1}$  for  $c > 0$ . Let us define  $z = |z|e^{i\delta}$ . Using (11) the condition  $-\pi < \delta < \pi$  can be directly translated to conditions on  $\beta_0$  and  $c$ , and therefore further division of the  $c$  axis is suggested as follows:

- (a) for  $c < -\beta_0 < 0$  we have  $\delta = -(\beta_0/c)\phi$ , and for  $\phi \in (-\pi, \pi)$  we always have  $-\pi < -|\beta_0/c|\pi < \delta < |\beta_0/c|\pi < \pi$ . Thus  $W_0(z)$  is the only relevant branch, its boundary is never reached and no singularity is encountered. We conclude that here the coupling has a perturbative fixed-point at  $x_{\text{FP}} = -1/c$ , and an analyticity structure that is consistent with causality.
- (b) for  $-\beta_0 < c < 0$ , we find that  $\delta = -(\beta_0/c)\phi$  reaches  $\pm\pi$  at  $\pm\phi_0$ , with

$$\phi_0 \equiv |c/\beta_0| \pi. \quad (14)$$

Thus, when  $Q^2$  has a phase of  $\pm\phi_0$ , the boundary of the  $W_0(z)$  branch is reached. Consequently, an image of the cut  $z \in (-\infty, -1/e)$  appears on the

first sheet in the  $Q^2$  plane. The branch point corresponding to  $z = -1/e$  appears at

$$Q^2 = Q_0^2 e^{\pm i\phi_0} \quad (15)$$

where

$$Q_0^2 = \Lambda^2 |c|^{-c/\beta_0}. \quad (16)$$

The cuts in the  $Q^2$  plane and the analytical continuation for  $|\phi| > \phi_0$  will be discussed later.

- (c) for  $c > \beta_0/2$ , the solution is given by  $W_{-1}(z)$  with  $\delta = +\pi - (\beta_0/c)\phi$  for  $\phi > 0$  and by  $W_1(z)$  with  $\delta = -\pi - (\beta_0/c)\phi$  for  $\phi < 0$ . For  $\phi \in (0, \pi)$ ,  $\delta > (1 - \beta_0/c)\pi$  and therefore it never reaches the  $W_{-1}$  branch boundary at  $\delta = -\pi$ . Similarly, for  $\phi \in (-\pi, 0)$ ,  $\delta < (-1 + \beta_0/c)\pi$  and therefore it never reaches the  $W_1$  branch boundary at  $\delta = +\pi$ . Thus, the only relevant branches are  $W_{\pm 1}$  and the only singularity encountered is the one at  $z = -1/e$  with the cut  $z \in (-\infty, -1/e)$  that separates between  $W_1$  and  $W_{-1}$ . From (11) we find that the  $z = -1/e$  singularity appears on the positive real  $Q^2$  axis, at  $Q^2 = Q_0^2$ , where  $Q_0^2$  is given in (16). The cut  $z \in (-\infty, -1/e)$  corresponds to a cut on the infrared section of the positive real  $Q^2$  axis,  $Q^2 \in (0, Q_0^2)$ .
- (d) for  $0 < c < \beta_0/2$ ,  $\delta = \pm\pi - (\beta_0/c)\phi$  and the boundary of  $W_{-1}$  at  $\delta = -\pi$ , and that of  $W_1$  at  $\delta = \pi$ , is reached at  $\phi = \pm\phi_1$ , where  $\phi_1 = 2(c/\beta_0)\pi$ . Like in case (b) above, it is required to define  $W(z)$  for  $\phi > \phi_1$ . This will be done soon.

In the two cases with large  $|\beta_0/c|$ , (b) and (d) above, we found that the boundary of the physical branch is reached, and therefore a definition of  $W(z)$  in eq. (11) for  $|\phi| > \phi_0$ , in (b), and  $|\phi| > \phi_1$ , in (d), is required. The criterion that  $W(z)$  should be continuous as a function of  $\phi$  for large  $|Q^2|$  implies a particular definition for the analytical continuation of  $W(z)$ : starting with a given branch  $W_{|n|}(z)$  and increasing  $|\phi|$ , then when the branch boundary is reached one switches to the next branch  $W_{|n|+1}(z)$ .

Let us illustrate the above starting with the case  $0 < c < \beta_0/2$ , (d) above, and consider a gradual increase in  $|\phi|$ , the phase of  $Q^2$ , in the lower half-plane  $\phi < 0$ . For a positive real  $Q^2$ ,  $z < 0$  and  $W(z)$  is just on the boundary between  $W_{-1}$  and  $W_1$ , shown by the dashed line in fig. 1. For a small negative  $\phi$ ,  $z$  is slightly below the negative real axis ( $\delta = -\pi - (\beta_0/c)\phi$ ) and the solution is within the branch  $W_1(z)$ . This is exemplified in fig. 1 by the case  $g = 0.1$  ( $\phi = -0.1\pi$ ). When  $\phi = -\phi_1 = -2(c/\beta_0)\pi$ ,  $\delta = \pi$ ,  $z$  becomes negative real again, and so the cut  $z \in (-\infty, 0)$  which is the upper boundary of the  $W_1(z)$  branch is reached. Continuity of  $W(z)$  is obtained if, and only if  $W_2(z)$  is used for  $\phi < -\phi_1$ . In fig. 1, this is exemplified by the case  $g = 0.6$  ( $\phi = -0.6\pi$ ). Note that in the specific example given in fig. 1, the time-like axis  $\phi = -\pi$  is reached within the  $W_2$  branch (the dot-dash line), but in general, depending on the ratio  $\beta_0/c$ , higher branches of  $W$  may become relevant.

Next, consider the case  $-\beta_0 < c < 0$ , (b) above, where the positive real  $Q^2$  solution is the positive real  $W$  axis in the  $W_0$  branch, described by the  $g = 0$  line in fig. 2. For a small negative  $\phi$ ,  $\delta = -(\beta_0/c)\phi$  is still far from the  $\delta = -\pi$  limit and the solution is given by  $W_0(z)$ . In fig. 2, this is exemplified by the case  $g = 0.1$  ( $\phi = -0.1\pi$ ). For  $\phi = -\phi_0 = (c/\beta_0)\pi$ , the cut at  $z = (-\infty, -1/e)$  which is the lower boundary of the  $W_0$  branch is reached. Continuity of  $W(z)$  at large  $|Q^2|$  (the right side of fig. 2) implies that for  $\phi \leq -\phi_0$ , the branch  $W_{-1}(z)$  should be used. In fig. 2 this is exemplified by the case  $g = 0.7$  ( $\phi = -0.7\pi$ ). The possibility that higher branches ( $W_{|n|}$  for  $n > 1$ ) will become relevant (depending on the ratio  $\beta_0/c$ ) exists also here. Just like in the previous case, these branches are reached through the  $z = 0$  cut.

A unique feature of the analytical continuation we perform appears in case (b) (see fig. 2): this is a “phase transition” from the Banks-Zaks non-trivial infrared fixed-point to the trivial one, that occurs at  $\phi = \pm\phi_0$ . For any  $|\phi| < \phi_0$  (the lines with  $g \leq 0.6$  in fig. 2)  $W(z)$  flows to zero in the infrared, which corresponds to the perturbative fixed-point at  $x_{\text{FP}} = -1/c$ . On the other hand, for any  $|\phi| > \phi_0$  (the lines with  $g \geq 0.7$  in fig. 2)  $|W(z)|$  becomes infinite in the infrared, which corresponds to  $x(Q^2) \rightarrow 0$ . The boundary between the  $W_0$  branch and the  $W_{-1}$  branch in fig. 2 separates between the two regimes. A flow from the ultraviolet down to the infrared for  $\phi = \phi_0$  ( $\phi = -(2/3)\pi$  in fig. 2) leads to a fork at  $W = -1$  (corresponding to  $Q^2 = Q_0^2$ ) from which there are two ways to continue towards  $Q^2 = 0$ , one is to the right, within the  $W_0$  branch leading to  $W = 0$ , and the other to the left, on the boundary between the  $W_{-1}$  and  $W_1$  branches, leading to  $W = -\infty$ . In other words, choosing the analytical continuation beyond  $|\phi| = \phi_0$  as we did, guarantees continuity for  $Q^2 \in (Q_0^2, \infty)$ , but leaves a discontinuity in the complex  $Q^2$  plane, along the  $\phi = \pm\phi_0$  directions for any  $Q^2 \in (0, Q_0^2)$ .

Let us now summarize how we choose the branch of the Lambert  $W$  function in (11) according to the proposed analytical continuation of the coupling to the entire complex  $Q^2$  plane. It is convenient to determine the branch from  $d \equiv -(\beta_0/c)\phi$ , where  $\phi$  is the phase of  $Q^2$ , as before<sup>§</sup>. Given  $d$ , we use the branch  $W_n$  such that for  $c < 0$ ,

$$d \in ((2n - 1)\pi, (2n + 1)\pi] \quad (17)$$

and for  $c > 0$ ,

$$\begin{aligned} d \in (2(n - 1)\pi, 2n\pi] \quad n \geq 1 \\ d \in (2n\pi, 2(n + 1)\pi] \quad n \leq -1 \end{aligned} \quad (18)$$

For instance, for  $c < 0$ ,  $W_{-1}$  is used for  $d \in (-3\pi, -\pi]$  and  $W_0$  is used for  $d \in (-\pi, \pi]$ , as shown in fig. 2. For  $c > 0$ ,  $W_1$  is used for  $d \in (0, 2\pi]$  and  $W_2$  is used for  $d \in (2\pi, 4\pi]$ , as shown in fig. 1.

Note that the lower half of the complex  $Q^2$  plane ( $\phi < 0$ ) always corresponds to a positive imaginary part for the coupling. For  $c < 0$  the lower half-plane corresponds

<sup>§</sup>Note that  $d$  is not the phase of  $z$ , since the latter has an additional  $\pi$  term for  $c > 0$ .



to  $d < 0$  which, according to (17), refers to  $n \leq 0$  i.e.  $\text{Im}\{W\} < 0$  that yields  $\text{Im}\{x(Q^2)\} > 0$  in (11). For  $c > 0$ ,  $\phi < 0$  corresponds to  $d > 0$  which according to (18) refers to  $n \geq 1$  i.e.  $\text{Im}\{W\} > 0$  that again yields  $\text{Im}\{x(Q^2)\} > 0$  in (11).

We are now in a position to address the question we started with, namely what is the singularity structure of  $x(Q^2)$  in the complex  $Q^2$  plane. There are three different possibilities, depending on the values of  $c$  and  $\beta_0 > 0$ , which are shown in fig. 3<sup>¶</sup>:

- (a) for  $c < -\beta_0 < 0$  the 2-loop coupling has a non-trivial perturbative infrared fixed point at  $x_{\text{FP}} = -1/c$  and an analyticity structure that is consistent with causality. Note there is no pole in the denominator of (11), since whenever  $W$  is real, it is positive. From considering only the 2-loop  $\beta$  function it is not possible to exclude the physical relevance of this fixed-point, and there is no indication of the existence of non-perturbative effects.
- (b) for  $-\beta_0 < c < 0$  the  $\beta$  function seems to have a fixed-point, as in a), but since  $x_{\text{FP}} = -1/c$  is large here, this fixed-point is probably not reliable – it can be washed out by higher-loop contributions or by non-perturbative effects. Existence of the latter is strongly suggested by the presence of causality violating singularities: there are two branch points at  $Q^2 = Q_0^2 e^{\pm i\phi_0}$  with radially oriented cuts that end at  $Q^2 = 0$ . The pole in the denominator of (11) at  $W = -1$  falls right on top of these branch points.
- (c) for  $c > 0$  there is no infrared fixed-point. The singularity structure violates causality, due to the branch point on the space-like axis at  $Q^2 = Q_0^2$ . The pole in the denominator of (11) at  $W = -1$  falls right on top of this branch point. Note that for  $c > 0$  it is not important whether  $\beta_0/c$  is large or small: in any case the only singularity is the single image of the  $z = -1/e$  branch point, the starting point of the cut that separates between  $W_1$  and  $W_{-1}$  (There are no similar singularities for higher branches  $|n| \geq 2$  of the  $W$  function). The non-physical cut on the space-like axis is probably removed from any physical quantity by non-perturbative effects.

The truncated 2-loop  $\beta$  function (7) can be considered as a legitimate choice of renormalization scheme – the so-called ‘t Hooft scheme. However, in certain cases this may be a peculiar choice of scheme for calculating observable quantities: the truncation of the  $\beta$  function at the 2-loop order seems quite arbitrary. Therefore, it is interesting to see to what extent our solution depends on this specific choice of scheme.

---

<sup>¶</sup>Some of these conclusions have been anticipated by Uraltsev [19].

## 4 The Lambert W solution at 3-loops

Given the above motivation we would like to generalize our results by considering a generic 3-loop RG equation:

$$\beta(x) = \frac{dx}{dt} = -\beta_0 x^2 (1 + cx + c_2 x^2) \quad (19)$$

where again  $t = \ln(Q^2/\Lambda^2)$ . A straightforward integration of (19) yields a function that involves arctanh terms in addition to the terms of the form appearing in (9). Therefore, it is even harder to explicitly invert this function. To avoid this difficulty, we use the following trick: we alter the 3-loop  $\beta$  function slightly, by taking its  $x^2[1/1]$  Padé Approximant (PA)<sup>||</sup>:

$$\beta_{PA}(x) = -\beta_0 x^2 \frac{1 + [c - (c_2/c)]x}{1 - (c_2/c)x} \quad (20)$$

This change does not limit generality as long as we restrict our interest to 3-loops, since the difference between the  $\beta$  function in (20) and that in (19) is of the order  $\mathcal{O}(x^4)$ . Indeed, using (20) instead of (19) is expected to change the singularity structure of  $x(Q^2)$ , but we insist that (20) corresponds to a choice of scheme at 4-loops and beyond which is just as arbitrary as the truncation in (19). Using (20) we obtain:

$$\beta_0 \ln(Q^2/\Lambda^2) = \frac{1}{x} - c \ln \left[ \frac{1}{x} + c - \frac{c_2}{c} \right] \quad (21)$$

and finally,

$$x(Q^2) = -\frac{1}{c} \frac{1}{1 - (c_2/c^2) + W(z)} \quad (22)$$

$$z = -\frac{1}{c} \exp \left[ -1 + (c_2/c^2) - \beta_0 t/c \right].$$

Just like in the 2-loop case (11), the sign of  $z$  and therefore also the physically relevant branch of  $W(z)$  are determined according the sign of  $c$ : for  $c > 0$ ,  $z < 0$  and the physical branch is  $W_{-1}(z)$ , taking real values in the range  $(-\infty, -1)$ , while for  $c < 0$ ,  $z > 0$  and the physical branch is  $W_0(z)$ , taking real values in the range  $(0, \infty)$ .

Note, that the only significant difference between the 3-loop solution (22) and the 2-loop solution (11) is in the relation between  $W(z)$  and  $x(Q^2)$ . This is because the difference in the definition of  $z$  can be swallowed in a redefinition of the scale parameter

$$\Lambda^2 \longrightarrow \tilde{\Lambda}^2 = \Lambda^2 e^{c_2/(\beta_0 c)}. \quad (23)$$

Consequently, we immediately know almost everything concerning the singularity structure of the PA-improved 3-loop coupling: it has the same type of branch points and cuts that are described in fig. 3. The difference is, however, that the simple

---

<sup>||</sup>PA's were found useful in various applications in perturbative QCD – see refs. [14, 20].

pole due to a zero in the denominator of  $x(Q^2)$  in (22) at  $W(z) = c_2/c^2 - 1$ , is not obtained on top of the branch point(s) at  $W = -1$  (which corresponds instead to the pole of the PA improved  $\beta$  function). Let us consider the three possible cases:

- (a) If  $c > 0$  then when  $W$  is real ( $W = W_{-1}$ ) it obeys  $W(z) < -1$  and then any  $c_2 < 0$  would result in a pole on the space-like axis.
- (b) If  $c < -\beta_0$  then when  $W$  is real ( $W = W_0$ ) it obeys  $W(z) > 0$  and then if  $c_2 > c^2$  the pole will appear on the space-like axis (for  $c_2 < c^2$  the coupling is causal) .
- (c) If  $-\beta_0 < c < 0$ ,  $W$  obtains (or approaches) any real value:  $W = W_0 \in (0, \infty)$  on the space-like axis,  $W \rightarrow W_0 \in (-1, 0)$  for  $|\phi| \rightarrow \phi_0^-$  and  $W \rightarrow W_{\pm 1} \in (-\infty, -1)$  for  $|\phi| \rightarrow \phi_0^+$ . Therefore for  $-\beta_0 < c < 0$ , the pole will always appear, either on the space-like axis (if  $c_2 > c^2$ ), or at  $|\phi| = \phi_0$  (if  $c_2 < c^2$ ).

We conclude that the singularity structure of the PA-improved 3-loop coupling is not much different from the 2-loop coupling: there are regions of the parameter space for which perturbative freezing is consistent with causality. In particular, this is true for small enough  $\beta_0$  and  $c < 0$ , which is the starting point for the Banks-Zaks expansion. In general, however, higher-order terms in the  $\beta$  function create a more complicated singularity structure in the infrared region, which is inconsistent with the analyticity requirement.

## 5 The Analytic Perturbation Theory approach

Recently it was suggested [4] to construct a causal coupling constant by analytically continuing the coupling to the time-like axis (i.e. looking at  $x(Q^2 = -s)$  with  $s > 0$ ), use the discontinuity, or equivalently the imaginary part, to define a spectral function  $\beta_R(s)$  as in (5) and finally use the dispersive integral (6) to construct a new space-like coupling  $x_{\text{APT}}(Q^2)$ . APT stands for ‘‘Analytic Perturbation Theory’’ since in this approach  $x_{\text{APT}}(Q^2)$  has the required analyticity structure by construction, being defined through the dispersion relation (6).

The authors of refs. [4, 5] show that the APT coupling has some remarkable features such as a universal infrared limit of  $1/\beta_0$  which is almost independent of the renormalization scheme and of the order of the  $\beta$  function one starts with. A general argument for the universality of the APT infrared limit (for  $c > 0$ ) was also given in [7]. With the explicit expression for the 2-loop coupling in (7), we can now directly check these conclusions.

Before dealing with the 2-loop case, let us briefly review the APT results at 1-loop, where both the spectral function and  $x_{\text{APT}}$  can be easily obtained in a closed form. One starts with the 1-loop  $\beta$  function (1) and performs an analytical continuation by substituting  $Q^2 = -s - i\epsilon$  where  $s > 0$  and  $\epsilon > 0$  is small. In the

limit  $\epsilon \rightarrow 0$  one obtains,

$$\begin{aligned}\text{Im}\{x(-s)\} &= \frac{\beta_0\pi}{(\beta_0\pi)^2 + (\beta_0t)^2} \\ \text{Re}\{x(-s)\} &= \frac{\beta_0t}{(\beta_0\pi)^2 + (\beta_0t)^2}\end{aligned}\quad (24)$$

where  $t \equiv \ln(s/\Lambda^2)$ . The spectral density is

$$\beta_R(t) = -\frac{1}{\pi}\text{Im}\{x(-s)\} = -\frac{1}{\beta_0\left[(\ln(s/\Lambda^2))^2 + \pi^2\right]}.\quad (25)$$

Finally, one constructs the corresponding space-like effective coupling, through the dispersion relation (6). The integral can be performed analytically, and yields

$$x_{\text{APT}}(Q^2) = \frac{1}{\beta_0}\left[\frac{1}{\ln(Q^2/\Lambda^2)} + \frac{\Lambda^2}{\Lambda^2 - Q^2}\right].\quad (26)$$

The first term in (26) is just the 1-loop perturbative result and the second term exactly cancels the ‘‘Landau-pole’’. Since the second term is a power correction, it does not alter the ultraviolet behavior. By construction,  $x_{\text{APT}}(Q^2)$  has a cut at  $\text{Re}\{Q^2\} < 0$  and no other singularities in the complex plane, and is therefore consistent with causality. The coupling has a non-perturbative infrared fixed-point at  $x_{\text{APT}}(0) = 1/\beta_0$ .

It is clearly of interest to see how these APT results change at 2-loops. Since we already know how to analytically continue the space-like coupling to the entire  $Q^2$  plane, we can now examine  $x(Q^2)$  on the time-like axis. Before doing so, we stress once more that for the uniqueness of the APT solution it is necessary to impose a continuity condition on  $x(Q^2)$  for large  $|Q^2|$ . This condition is implemented by starting from  $x(Q^2)$  on the space-like axis with  $Q^2 \gg \Lambda^2$ , and demanding continuity of  $x(Q^2)$  as the phase of  $Q^2$  is changed. This prescription is essential, since the naive alternative of ‘‘taking a shortcut’’ and going directly to the time-like axis by trying to invert (9) for negative  $Q^2$  leads to an ambiguity in the choice of the branch of  $W$  and in the corresponding APT spectral function.

Actually, perturbatively speaking, there can be no ambiguity in the definition of  $x(Q^2)$  at complex  $Q^2$ . To see this one first writes the solution of eq. (4) in the standard ‘‘non-improved’’ way as  $x(Q^2/\mu^2, x_0)$ , where  $x_0 \equiv x(Q^2 = \mu^2)$ , and expands in powers of  $x_0$ . The resulting coefficients are polynomials in  $\log(Q^2/\mu^2)$  (the standard RG logs) and can all be expressed in terms of the  $\beta$  function coefficients. If the  $\beta$  function is given by a convergent power series (as in all examples we examine here), then the resulting series for  $x(Q^2/\mu^2, x_0)$  has a *finite* radius of convergence at any fixed  $|Q^2/\mu^2|$ , and defines the unique correct analytic continuation to complex  $Q^2$ . Given the finite convergence radius, there are no singularities for a fixed  $|Q^2/\mu^2|$  if  $x_0$  is small enough. Due to asymptotic freedom, small enough  $x_0$  at fixed  $|Q^2/\mu^2|$  corresponds to large  $|Q^2|$  and therefore  $x(Q^2)$  has no singularities for large enough  $|Q^2|$ .

Considering the 2-loop APT spectral function,  $\beta_R(t) = -(1/\pi) \text{Im}\{x(-s - i\epsilon)\}$  with  $x(Q^2)$  given by eq. (11), we show in fig. 4 the values of  $W$  along the time-like axis, below the cut, for a 2-loop  $\beta$  function with  $\beta_0 = 1$  and several different values of  $c$ . We identify two categories of lines in fig. 4:

- (a) for  $c < -\beta_0$  ( $c < -1$  in the figure)  $W$  flows to zero in the infrared. This leads to a non-trivial perturbative infrared fixed-point:  $x(Q^2) \rightarrow x_{FP} = -1/c$ .
- (b) for  $c > -\beta_0$  (where  $c$  can be either positive or negative)  $|W| \rightarrow \infty$  in the infrared, and thus  $x(Q^2) \rightarrow 0$ .

When  $c < -\beta_0$ , the singularity structure (see fig. 3) is consistent with causality: the cut is only on the time-like axis. This guarantees that  $x(Q^2)$  obeys the dispersion relation in eqs. (5) and (6). It follows that in this case the APT coupling coincides with the perturbative coupling:  $x_{\text{APT}}(Q^2) = x(Q^2)$ . On the other hand, when  $c > -\beta_0$ , the singularity structure is always inconsistent with causality (see fig. 3). Therefore in this case  $x_{\text{APT}}(Q^2)$  differs from the perturbative coupling  $x(Q^2)$ .

Having identified how the relative size of  $c$  vs.  $\beta_0$  affects the main features of the APT coupling, we are now ready to consider the actual 2-loop  $\beta$  function in QCD and examine the dependence of the analytically continued coupling  $x(-s)$  on  $N_f$ , the number of light quark flavors. In fig. 5 we plot values of  $W$  along the time-like axis, below the cut, for  $N_f = 0, 1, 2, \dots, 16$ . As already mentioned, the branch  $W_n$  in which the solution corresponding to the time-like axis resides, depends on  $c/\beta_0$ . The table below lists the values of  $N_f$ , and the corresponding branch labels  $n$ .

$N_f$	0	1	2	3	4	5	6	7	8	9	10	11	12	13	14	15	16
$n$	1	1	1	1	1	1	1	2	25	-1	0	0	0	0	0	0	0

For  $N_f \geq 10$  we have  $c < -\beta_0$ , so the APT coupling coincides with the perturbative one. On the other hand, for  $N_f \leq 9$  we have  $c > -\beta_0$ , and then we expect the APT solution to be different. For  $N_f = 9$ ,  $-\beta_0 < c < 0$  and therefore a pair of complex singularities appears, while for  $N_f \leq 8$  there is a single singularity of the space-like axis. The  $N_f = 8$  line is not shown in fig. 5, since the large value of  $\beta_0/c$  in this case causes the corresponding  $\text{Im}(W)$  to fall within the  $W_{25}$  branch, way outside the vertical range of the plot. It is important to note that for the physically relevant case,  $N_f \leq 3$ , the exact number of flavours has only a small effect on  $W$ .

Next, we use (11) to calculate  $x(-s)$  below the cut for two representative examples:  $N_f = 3$  and  $N_f = 10$ . The corresponding real and imaginary parts of  $x(-s)$  are shown in fig. 6 as function of  $t = \ln(s/\Lambda^2)$ . The ultraviolet limit of the real part is the same in both cases:  $\text{Re}\{x(-s)\} \rightarrow 0$ . The difference is in the infrared: for  $N_f = 10$ ,  $\text{Re}\{x(-s)\} \rightarrow x_{FP} = -1/c$ , in accordance with (a) above, while for  $N_f = 3$ ,  $\text{Re}\{x(-s)\} \rightarrow 0$ , in accordance with (b) above. The imaginary part of  $x(-s)$  vanishes in both the infrared and in the ultraviolet limit, so that the APT coupling given by (5) and (6) is well defined.

$\text{Im}\{x(-s)\}$  below the cut is always positive-definite and thus the APT coupling is a monotonically decreasing function of  $Q^2$ , attaining its maximum value  $x_{\text{APT}}(0)$

at  $Q^2 = 0$ . The infrared limit of the APT coupling can be obtained by integrating  $\text{Im}\{x(-s)\}$  over all scales:

$$x_{\text{APT}}(0) = \frac{1}{\pi} \int_{-\infty}^{\infty} \text{Im}\{x(-s)\} dt \quad (27)$$

This integral can be performed analytically by changing the integration variable to  $W$ . Using (10) and (11) we write  $dt = (-c/\beta_0)(1+W)/W dW$  and obtain:

$$x_{\text{APT}}(0) = \frac{1}{\beta_0} \frac{1}{\pi} \text{Im} \left\{ \int_{\text{IR}}^{\text{UV}} \frac{dW}{W} \right\} \quad (28)$$

where the integration contour in the  $W$  plane is along the line that corresponds to the *time-like* axis (examples are provided by the continuous lines in figs. 4 and 5).

For  $c > 0$  and for  $-\beta_0 < c < 0$  the time-like axis is always mapped into a non-principle branch ( $n \neq 0$ ) and then the integration contour stretches from  $\text{Re}\{W\} \rightarrow -\infty$  to  $\text{Re}\{W\} \rightarrow +\infty$ , while  $\text{Im}\{W\}$  is bounded. The integral can then be performed by closing the integration contour with a semi-circle at infinity. Since there are no poles inside the closed contour and the integration along the semi-circle yields  $i\pi$ , one obtains  $x_{\text{APT}}(0) = 1/\beta_0$ .

For  $c < -\beta_0$  the relevant branch is  $n = 0$  and then the contour starts at  $W = 0$  in the infrared and reaches  $\text{Re}\{W\} \rightarrow +\infty$  in the ultraviolet. In this case we evaluate the integral directly and then use the asymptotic behavior of  $W_0(z)$  at small and large  $|z|$ . The result is  $x_{\text{APT}}(0) = -1/c$ . A posteriori, this should not come as a surprise, since we already know that whenever the time-like coupling is within the  $W_0$  branch, ( $c < -\beta_0$ ), the APT solution coincides with the perturbative coupling which flows to the infrared fixed-point at  $-1/c$ .

We note that the conclusion of refs. [4, 5] that the infrared limit of the 2-loop APT coupling is always  $1/\beta_0$  is correct only for  $c > -\beta_0$ .

Our results for 2-loop  $x_{\text{APT}}(0)$  are summarized in fig. 7, where the upper plot (continuous line) shows the 2-loop APT infrared limit for a  $\beta$  function with  $\beta_0 = 1$  and a span of  $c$  values, and the lower plot (continuous line and crosses) shows the 2-loop APT infrared limit for QCD with a varying number of flavours. For  $N_f \leq 9$  the APT infrared limit is  $1/\beta_0$ , while for  $N_f \geq 10$  it is  $-1/c$ .

In a similar manner we now calculate the infrared APT limit for the PA-improved three-loop coupling defined from the imaginary part of  $x(-s)$  in eq. (22). Also here we perform the integral analytically by changing the integration variable to  $W$ ,

$$x_{\text{APT}}(0) = \frac{1}{\beta_0} \frac{1}{\pi} \text{Im} \left\{ \int_{\text{IR}}^{\text{UV}} \frac{W+1}{W+1-c_2/c^2} \frac{dW}{W} \right\}. \quad (29)$$

We find the same two scenarios: when the time-like axis corresponds to a non-principal branch, we close the contour by a half-circle at infinity. Otherwise, for  $n = 0$ , we evaluate the integral directly and use asymptotics of  $W_0(z)$ .

Depending on the values of  $\beta_0$ ,  $c$  and  $c_2$ , there are four different possibilities, as summarized below:

$$\begin{array}{r}
c > 0 \\
c < 0
\end{array}
\left\{ \begin{array}{l}
c > -\beta_0 \\
c < -\beta_0
\end{array} \right\}
\left\{ \begin{array}{l}
c_2 < c^2 \\
c_2 > c^2
\end{array} \right.
\begin{array}{l}
\underline{x_{\text{APT}}(0)} \\
1/\beta_0 \\
1/\beta_0 \\
(-1/c)/(1 - c_2/c^2) \\
1/\beta_0 - (1/c + 1/\beta_0)/(1 - c_2/c^2)
\end{array}
\quad (30)$$

For  $c > -\beta_0$  we again obtain a completely universal infrared limit:  $x_{\text{APT}}(0)$  does not depend at all on  $c$  and  $c_2$ . The universality breaks down for  $c < -\beta_0$ , just like in the two-loop case. When the singularity structure of the perturbative coupling is consistent with causality, we expect that it coincides with the APT coupling, and then  $x_{\text{APT}}(0)$  should be just equal to the solution of  $\beta(x) = 0$ , which is  $x(Q^2 = 0) = (-1/c)/(1 - c_2/c^2)$ . However, contrary to the two-loop case, at three-loops, given  $c < -\beta_0$ , it is still possible that the singularity structure will be inconsistent with causality: if  $c_2 > c^2$  the perturbative coupling has an extra pole on the space-like axis (see discussion below eq. (23), case (b)). Indeed, in this case the APT infrared limit is different from the perturbative one.

Our results for the infrared limit of the APT coupling at 3-loops are shown in fig. 7, on top of the 2-loop results. The plot demonstrates that as long as  $c > -\beta_0$  the limit  $x_{\text{APT}}(0) = 1/\beta_0$  is universal, i.e. it does not depend on  $c$  and  $c_2$ . Nevertheless, when  $c < -\beta_0$  the values of  $c$  and  $c_2$  are important for the APT infrared limit, as indicated by (30).

In the upper plot, one notes that for a 3-loop case with  $c_2 > 0$  and  $c < 0$ ,  $x_{\text{APT}}(0)$  can become large, and even diverge, when  $c_2 \sim c^2$ . Then  $x_{\text{APT}}$  ceases to be a good expansion parameter. Another interesting feature of the 3-loop solution is the jump that may occur in the value of  $x_{\text{APT}}(0)$  at  $c = -\beta_0$  when  $c$  is varied. Such a jump indeed occurs if  $c_2 < c^2$  (dashed line in the upper plot).

In the lower plot, one observes that the APT coupling based on the PA-improved 3-loop  $\beta$  function in  $\overline{\text{MS}}$  shows a sharp transition at  $N_f \simeq 10$ . For  $N_f \geq 10$  the coupling has a perturbative infrared fixed point at a rather small value ( $x(0) \sim 0.1$ ), suggesting a reliable purely perturbative phase. On the other hand, for  $N_f \leq 9$  the APT coupling has a non-perturbative infrared fixed point, with the ‘‘universal’’ value of  $1/\beta_0$ . It is natural to ask whether the transition observed at  $N_f \simeq 10$  is an indication of the phase transition expected in QCD as  $N_f$  is increased (see [3] and refs. therein), or is it an artifact of considering a truncated  $\beta$  function in a special renormalization scheme. While we cannot fully answer this question, it is worthwhile noting that the transition point  $N_f \sim 10$  does not depend on the renormalization scheme, since it reflects the *scheme-independent* condition  $c = -\beta_0$ . Moreover, the essential qualitative features of the  $\overline{\text{MS}}$  results for  $N_f \geq 10$  are likely shared by most acceptable renormalization schemes: one observes that in physical schemes the condition  $c_2 < c^2$  is always obeyed for  $N_f \geq 10$  (see fig. 1 in [3]). Therefore, the perturbative fixed-point of the PA-improved 3-loops  $\beta$  function at

$(-1/c)/(1 - c_2/c^2)$  is positive and the perturbative coupling has a causal analyticity structure. The last case considered in (30), i.e.  $c < -\beta_0$  and  $c_2 > c^2$ , is probably never realized in QCD.

## 6 Summary and Conclusions

Using the Lambert  $W$  function we achieved a thorough understanding of the structure of the solutions of the 2-loop and (Padé improved) 3-loop RG equation for the coupling constant in the complex  $Q^2$  plane. The main result is that the running perturbative coupling in QCD can have a causal analyticity structure, with a non-trivial infrared fixed point, provided  $\beta_0$  is small enough and that  $\beta_1$  is negative, i.e. in the framework of the Banks-Zaks expansion. This suggests that a consistent, purely perturbative definition of QCD should be possible when the number of flavors is large enough (barring possible complications due to renormalons and to the asymptotic nature of the  $\beta$  function series and of the Banks-Zaks series, which have not been addressed here). On the other hand, for larger  $\beta_0$  or for positive  $\beta_1$ , unphysical singularities are present in the infrared region, which are to be removed by non-perturbative power-like effects.

At the 2-loop level, the causality requirement translates into the condition  $\beta_1 < -\beta_0^2$ , i.e.  $x_{FP} \equiv -1/c < 1/\beta_0$ . This condition is also relevant for the PA-improved 3-loop case, for most of the acceptable renormalization schemes. Taking seriously the 2-loop and 3-loop results, we are lead to conclude that a purely perturbative phase is realized in QCD with  $N_f \geq 10$ . This result is in reasonable agreement with other approaches (see [3] and refs. therein).

We have investigated the APT approach, a simple mathematical way (which admittedly lacks a physical basis, see the discussion below) to implement the necessary power-like effects, starting from perturbation theory. In this approach, a causal coupling is reconstructed via a dispersion relation from the time-like discontinuity of the *perturbative* coupling. We have shown that in some cases the value of the APT infrared fixed point may depend on higher-order coefficients of the perturbative  $\beta$  function, and is not always given by the one-loop value  $1/\beta_0$ , which is therefore not “universal”. Departure from the “universal” value appears not only in the above mentioned cases where the perturbative coupling is by itself already causal and the APT fixed point coincides with the perturbative one, but also when unphysical space-like singularities are present and a (positive) perturbative infrared fixed point does not exist – case (b) below eq. (23). Nevertheless, the latter case might be viewed as academic, since in QCD it is not realized for any number of flavors.

It is therefore natural to wonder what general conditions are required to recover the “universal” APT value, which clearly has a special, remarkable status (in particular, all the “non-perturbative” APT fixed point curves end up on the “universal”  $1/\beta_0$  line in Fig.(7)). Sufficient conditions for the “universal” APT value were given in [7], *assuming* a Landau singularity is present on the space-like axis:



essentially, the perturbative coupling was required to approach the *trivial* infrared fixed point when the scale is decreased to zero on the *space-like* axis below the Landau singularity<sup>\*\*</sup>. Thus, in order to avoid universality in this case, there must exist a *non-trivial*, but *perturbative*, infrared fixed point (at unphysical negative or complex values of the coupling), whose domain of attraction includes the trajectory going through the Landau singularity. Indeed, a (negative) perturbative infrared fixed point is present in the 3-loop example for  $c < 0$  and  $c_2 > c^2$ , explaining why the last “non-perturbative” APT fixed point in eq. (30) differs from the “universal” value. Actually, universality may be obtained under more general conditions than those stated in [7], e.g. in the case  $-\beta_0 < c < 0$  in eq. (30), where the APT value is still the universal one, despite the presence of a non-trivial perturbative infrared fixed point (which always exists for  $c < 0$ ), and regardless of its sign (if the latter is negative, then a Landau pole is still present on the space-like axis).

In all the examples presented here, namely the 2-loop and PA-improved 3-loop  $\beta$  functions, universality is obtained whenever the perturbative coupling approaches the *trivial* infrared fixed point as  $Q^2 \rightarrow 0^-$  on the *time-like* axis. This has a simple mathematical explanation in terms of the Lambert W function, as in these cases, the contour in the  $W$  plane stretches from  $\text{Re}\{W\} \rightarrow -\infty$  to  $\text{Re}\{W\} \rightarrow +\infty$ , while  $\text{Im}\{W\}$  is bounded. The integral can then be performed by closing the integration contour with a semi-circle at infinity. Since there are no poles inside the closed contour and the integration along the semi-circle yields  $i\pi$ , one obtains  $x_{\text{APT}}(0) = 1/\beta_0$ . As a result, the details of the contour, which do depend on the coefficients of the  $\beta$  function, are insignificant.

It would be interesting to know whether, for a *generic* higher-order  $\beta$  function, a universal  $1/\beta_0$  limit of the APT coupling is obtained whenever the perturbative coupling approaches the *trivial* infrared fixed point on the *time-like* axis, giving a sufficient condition for universality alternative to that of [7]. Unfortunately, because of the complicated phase structure in the complex  $Q^2$  plane when complex Landau singularities are present (see the discussion before eq. (17)), it is not clear if such a condition could turn out to be also necessary. Note that in the present examples, for  $-\beta_0 < c < 0$  there is a 2-phase structure, such that the space-like coupling approaches the non-trivial perturbative infrared fixed point, while the time-like coupling approaches the trivial one. On the other hand, for  $c < -\beta_0 < 0$  there is only one phase and both couplings approach the non-trivial fixed point. But, in principle, there could be more complicated examples where a third scenario is realised, namely the space-like coupling approaches the trivial fixed point (thus insuring universality according to [7]), while the time-like coupling approaches a non-trivial one.

It is also interesting to note that the PA-improved 3-loop coupling probably offers the simplest example (in case  $c < 0$  and  $c_2 > c^2$ ) where the standard relation between renormalons and Landau pole (see previous footnote) might not hold, since the Landau pole trajectory is not in the domain of attraction of the trivial infrared fixed point in this example. Developing this point is beyond the scope of the present

---

<sup>\*\*</sup>This condition also allows to relate [21] the ambiguity arising from integrating over the Landau singularity to the one due to renormalons, a fact exploited in the proof.

paper.

One might question the physical relevance of the APT coupling. It is unlikely, given its perturbative origin, that it exhausts all non-perturbative effects in the running coupling, but it may play a useful phenomenological role (yet to be clarified) in a more general framework [7, 22].

## Acknowledgments

This research was supported in part by the Israel Science Foundation administered by the Israel Academy of Sciences and Humanities, by a Grant from the G.I.F., the German-Israeli Foundation for Scientific Research and Development, by the Charles Clore doctoral fellowship, and by the EC program ‘Training and Mobility of Researchers’, Network ‘QCD and Particle Structure’, contract ERBFMRXCT980194.

## References

- [1] D. Gross and F. Wilczek, *Phys. Rev. Lett.* **30** (1973) 1343; H.D. Politzer *Phys. Rev. Lett.* **30** (1973) 1346.
- [2] V. I. Zakharov, *Renormalons as a bridge between perturbative and nonperturbative physics*, hep-ph/9802416.
- [3] E. Gardi, M. Karliner, *Relations between observables and the infrared fixed-point in QCD*, to be published in *Nucl. Phys.* **B**, hep-ph/9802218.
- [4] I.L. Solovtsov and D.V. Shirkov, *Phys. Rev. Lett.* **79** (1997) 1209-1212, *Analytic model for the QCD running coupling with universal  $\alpha_s(0)$  value* hep-ph/9704333.
- [5] D.V. Shirkov, *On the analytic “Causal” model for the QCD running coupling*, hep-ph/9708480; K. A. Milton, O. P. Solovtsova, OKHEP-97-06, *Analytic perturbation theory: a new approach to the analytic continuation of the strong coupling constant  $\alpha_s$  into the time-like region*, hep-ph/9710316; I.L. Solovtsov and D.V. Shirkov *Analytic approach to perturbative QCD and renormalization scheme dependence*, hep-ph/9711251; K. A. Milton, I.L. Solovtsov and O. P. Solovtsova, *Phys. Lett.* **B415** (1997) 104.
- [6] Yu.L. Dokshitzer, G. Marchesini and B.R. Webber, *Nucl. Phys.* **B469** (1996) 93.
- [7] G. Grunberg, *Power corrections and Landau singularity*, hep-ph/9705290.
- [8] R. Akhoury and V.I. Zakharov, UM-TH/97-11, hep-ph/9705318; UM-TH/97-19, hep-ph/9710257; UM-TH/97-18, hep-ph/9710487; G. Grunberg, CERN-TH/97-340, hep-ph/9711481.

- [9] W. E. Caswell, *Phys. Rev. Lett.* **33**, (1974) 244; D. R. T. Jones, *Nucl. Phys.* **B75**, (1974) 531.
- [10] T. Banks and A. Zaks, *Nucl. Phys.* **B196** (1982) 189. See also G. Grunberg, *Phys. Rev.* **D46**, (1992) 2228.
- [11] R.M. Corless, G.H. Gonnet, D.E.G. Hare, D.J. Jeffrey and D.E. Knuth, “On the Lambert W function”, *Advances in Computational Mathematics*, **5** (1996) 329, available from <http://pineapple.apmaths.uwo.ca/~rmc/papers/LambertW/>.
- [12] C. J. Maxwell, *Phys. Lett.* **B409** (1997) 450-454.
- [13] G. Cvetič, *Phys. Rev.* **D57** (1998) 3209-3213; G. Cvetič, *Nucl. Phys.* **B517** (1998) 506-520; see also G. Cvetič and R. Kögerler, MPI-PhT 98-13, BI-TP 98/2, hep-ph/9802248.
- [14] E. Gardi, *Phys. Rev.* **D56** (1997) 68; S. J. Brodsky, J. Ellis, E. Gardi, M. Karliner, M.A. Samuel. *Phys. Rev.* **D56** (1997) 6980-6992.
- [15] G. Grunberg, *Phys. Rev.* **D29** (1984) 2315.
- [16] P.M. Stevenson, *Phys. Rev.* **D23** (1981) 2916.
- [17] N.N. Khuri and H.C. Ren, *Annals Of Physics* **189** (1989) 142-154.
- [18] G. Grunberg, *Phys. Lett.* **B304** (1993) 183.
- [19] N.G. Uraltsev, private communication with G. Grunberg.
- [20] M.A. Samuel, J. Ellis and M. Karliner, *Phys. Rev. Lett.* **74** (1995) 4380; *Phys. Lett.* **B400** (1997) 176; J. Ellis, E. Gardi, M. Karliner and M.A. Samuel, *Phys. Lett.* **B366** (1996) 268; *Phys. Rev.* **D54** (1996) 6986; I. Jack, D.R.T. Jones and M.A. Samuel, hep-ph/9706249; J. Ellis, I. Jack, D.R.T. Jones, M. Karliner and M.A. Samuel, *Phys. Rev.* **D57** (1998) 2665.
- [21] G. Grunberg *Phys. Lett.* **B372** (1996) 121.
- [22] A.I. Alekseev, *QCD Running Coupling: Freezing Versus Enhancement in the Infrared Region*, hep-ph/9802372; A.I. Alekseev, B.A. Arbuzov, *Analyticity and Minimality of Non-perturbative Contributions in Perturbative region for  $\bar{\alpha}_s$* , hep-ph/9704228.

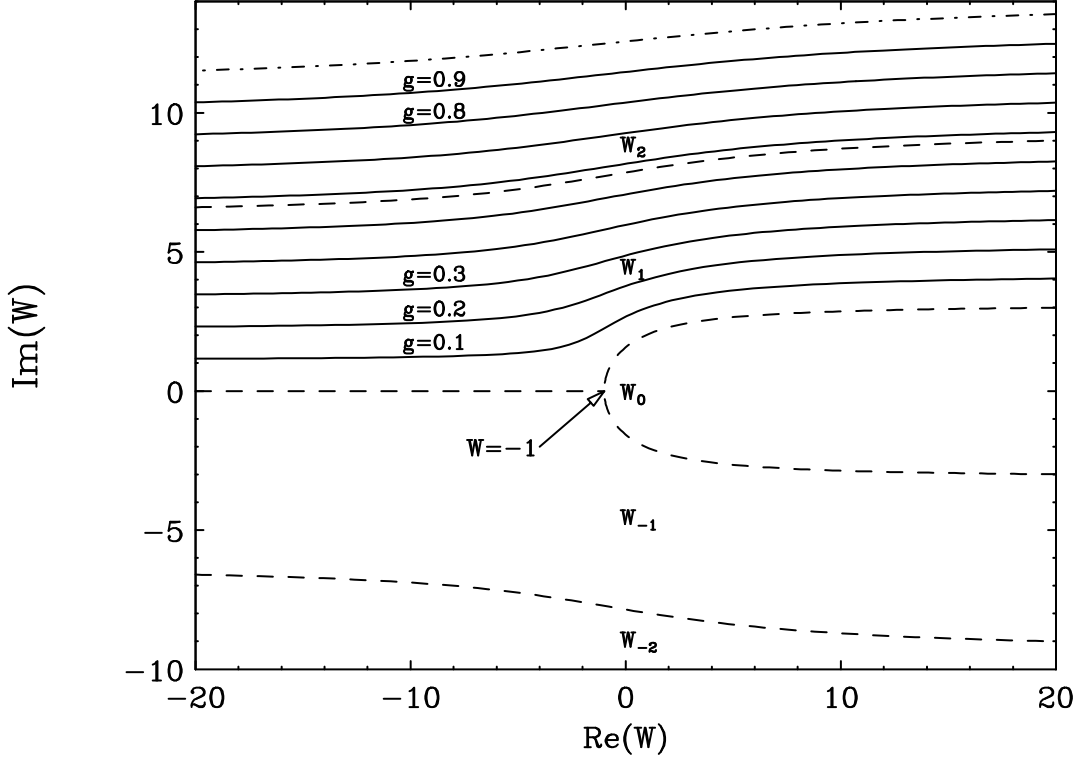


Figure 1: The complex  $W$  plane is divided by dashed lines to branches of the Lambert  $W$  function:  $W_0$ ,  $W_{\pm 1}$ ,  $W_{\pm 2}$ . The dashed line that forms the boundary between  $W_1$  and  $W_{-1}$  represents also the values of  $W$  for the space-like coupling at 2-loops for  $c > 0$  (above the Landau singularity). The continuous lines correspond to the values of  $W$  for a set of fixed phase rays in the lower  $Q^2$  half-plane for the example of a 2-loop  $\beta$  function with  $\beta_0 = 1$  and  $c = 2/7$ . Large  $|Q^2|$  corresponds to the left side of the lines, while the infrared limit corresponds the right side. The phases in the  $Q^2$  plane are  $\phi = -g\pi$ , where  $g = 0.1, 0.2, 0.3, \dots, 0.9$ . The dot-dashed line ( $g = 1$ ) corresponds to the time-like axis below the cut. The use of  $W_2$  for  $\phi < -\phi_1 = -2(c/\beta_0)\pi \simeq -0.571\pi$  guarantees the continuity of  $W$ .

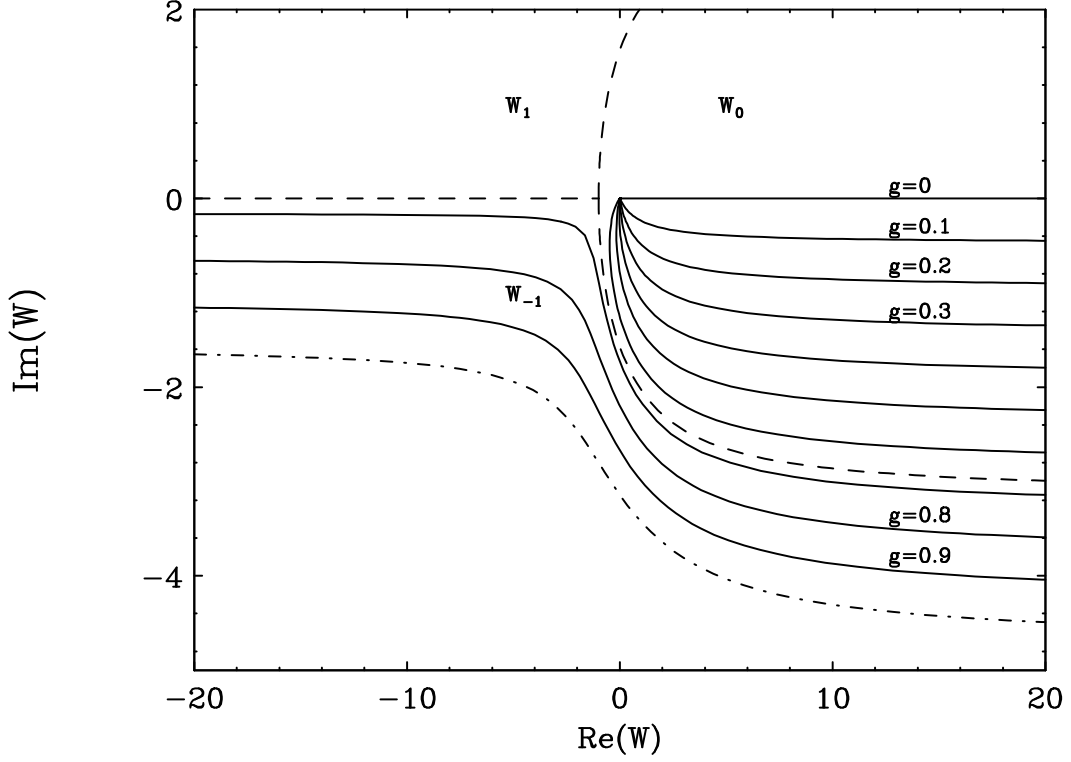


Figure 2: The complex  $W$  plane is divided by dashed lines to branches of the Lambert  $W$  function:  $W_0$  and  $W_{\pm 1}$ . The  $g = 0$  line corresponds to the values of  $W$  for the space-like coupling at 2-loops for  $c < 0$ . The rest of the continuous lines correspond to the value of  $W$  for a set of fixed phase rays in the lower  $Q^2$  half-plane for the example of a 2-loop  $\beta$  function with  $\beta_0 = 1$  and  $c = -2/3$ . Large  $|Q^2|$  corresponds to the right side of the lines. The phases in the  $Q^2$  plane are  $\phi = -g\pi$ , where  $g = 0.1, 0.2, 0.3, \dots, 0.9$ . The dot-dashed line ( $g = 1$ ) corresponds to the time-like axis below the cut. The use of  $W_{-1}$  for  $\phi < -\phi_0 = -|c/\beta_0|\pi \simeq -0.667\pi$  guarantees continuity of  $W$  for  $|Q^2| > Q_0^2$  (see eq. (16)).

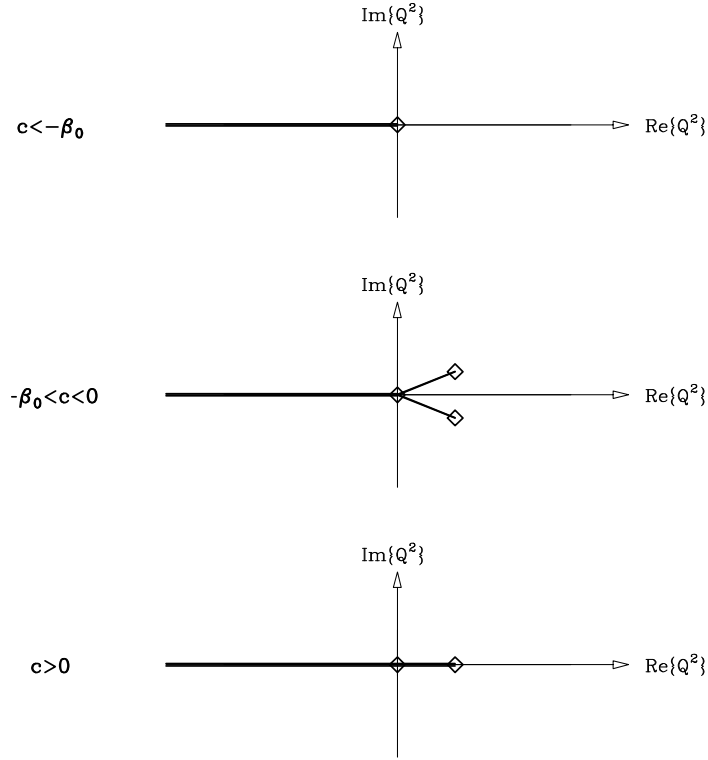


Figure 3: The three possibilities for the singularity structure of the 2-loop coupling. Branch points are represented by diamonds and cuts by bold lines. Only for  $c < -\beta_0$  (upper plot) perturbative freezing leads to a singularity structure that is consistent with causality. For  $-\beta_0 < c < 0$  there is a pair of complex conjugate branch points and for  $c > 0$  there is one space-like branch point that violate causality. Note that with the present analytical continuation, the non-causal singularities are confined to the infrared region, where they can be removed from physical quantities by non-perturbative effects.

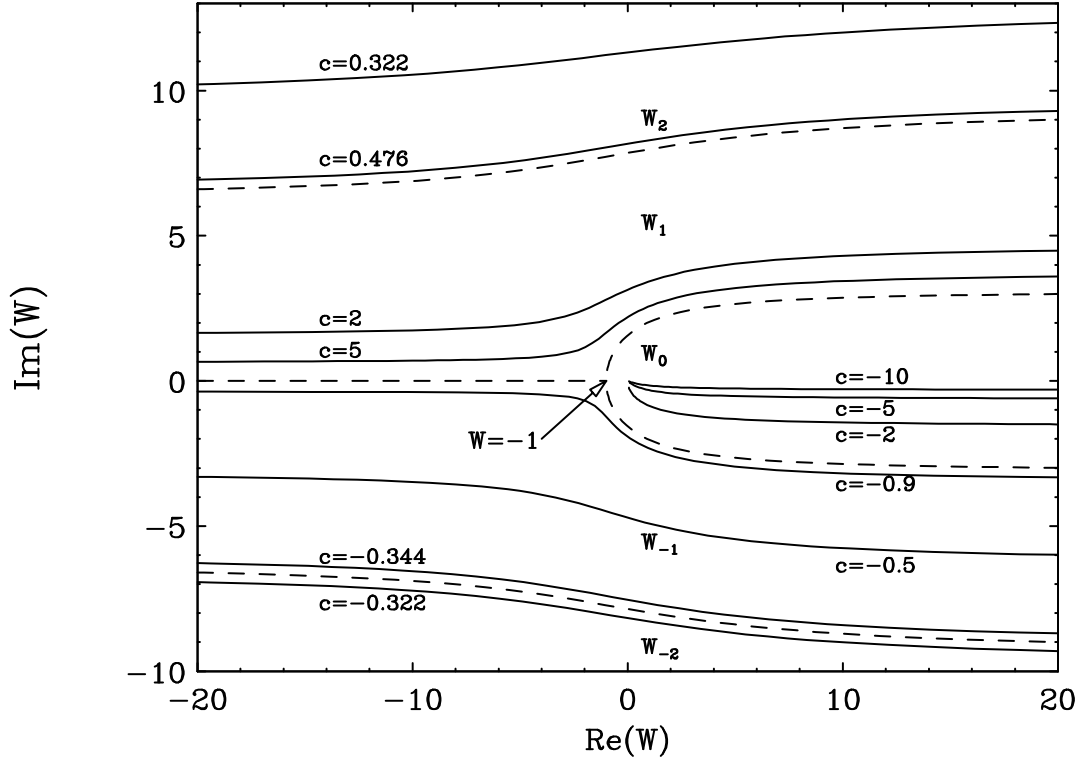


Figure 4: The various continuous lines show the value of  $W$  along the time-like axis (below the cut), corresponding to the 2-loop coupling for  $\beta_0 = 1$  and different values of  $c$ . For the  $c > 0$  large  $|Q^2|$  corresponds to the left side of the lines, while for  $c < 0$  large  $|Q^2|$  corresponds to the right side. The dashed lines show the division of branches of the Lambert  $W$  function:  $W_0$ ,  $W_{\pm 1}$  and  $W_{\pm 2}$ .

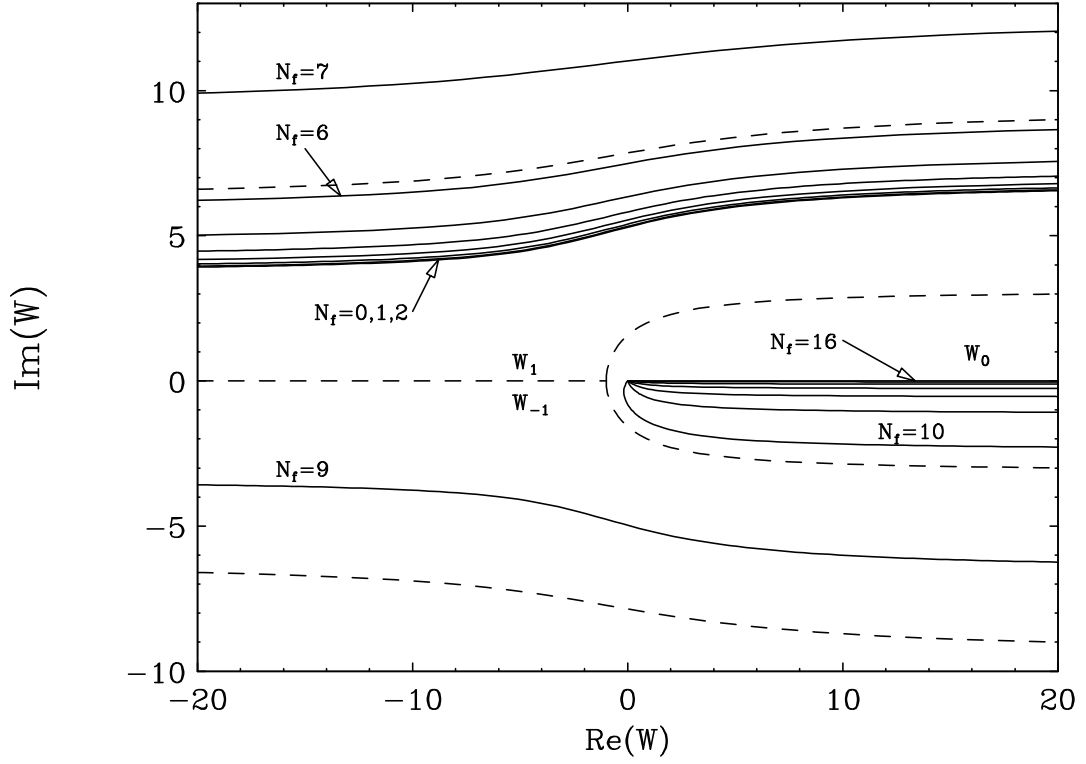


Figure 5: The various continuous lines show the value of  $W$  along the time-like axis (below the cut), corresponding to the QCD 2-loop coupling for different value of  $N_f = 0, 1, 2, \dots, 16$ . The dashed lines show the division of branches of the Lambert  $W$  function:  $W_0$  and  $W_{\pm 1}$ .



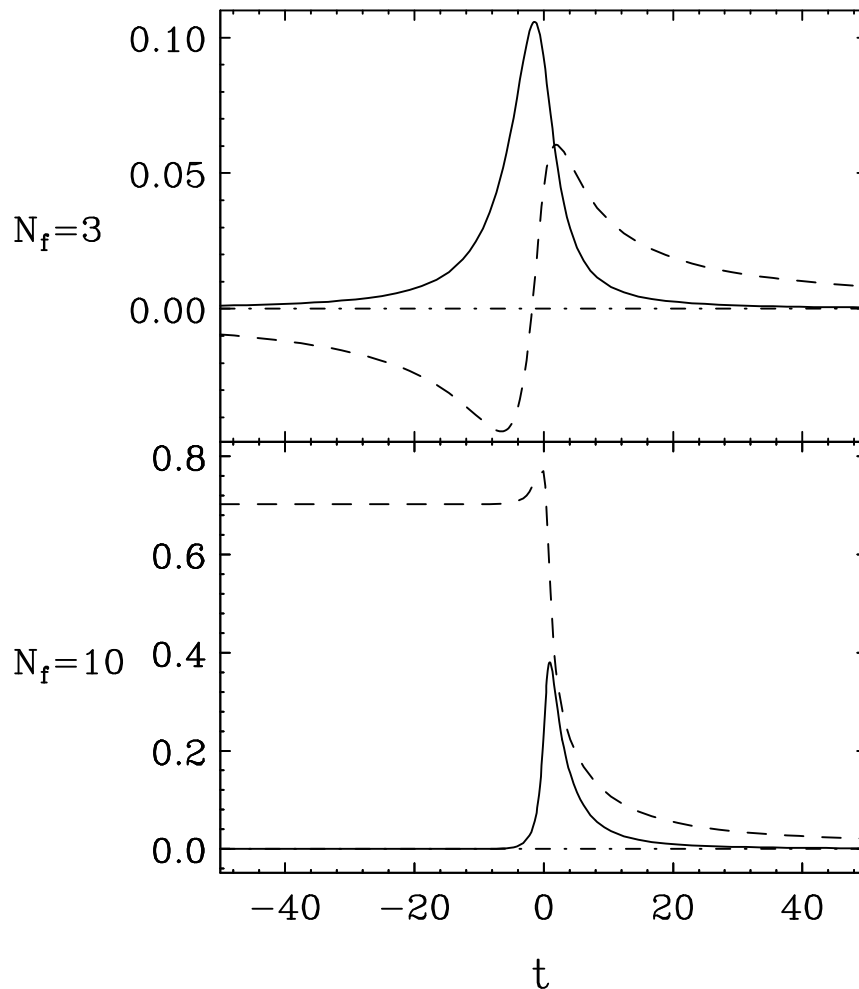


Figure 6: The real (dashed line) and imaginary (solid line) parts of the analytically continued coupling on the time-like axis,  $x(-s)$ , for the case of a 2-loop  $\beta$  function in QCD with  $N_f = 3$  ( $\beta_0 = 9/4$  and  $c = 16/9$ ) in the upper box, and  $N_f = 10$  ( $\beta_0 = 13/12$  and  $c = -37/26$ ) in the lower box. For  $N_f = 10$  perturbative freezing leads to a well defined infrared limit for the perturbative coupling:  $x^{FP} = -1/c$ , while for  $N_f = 3$  the “perturbative infrared limit” is zero.

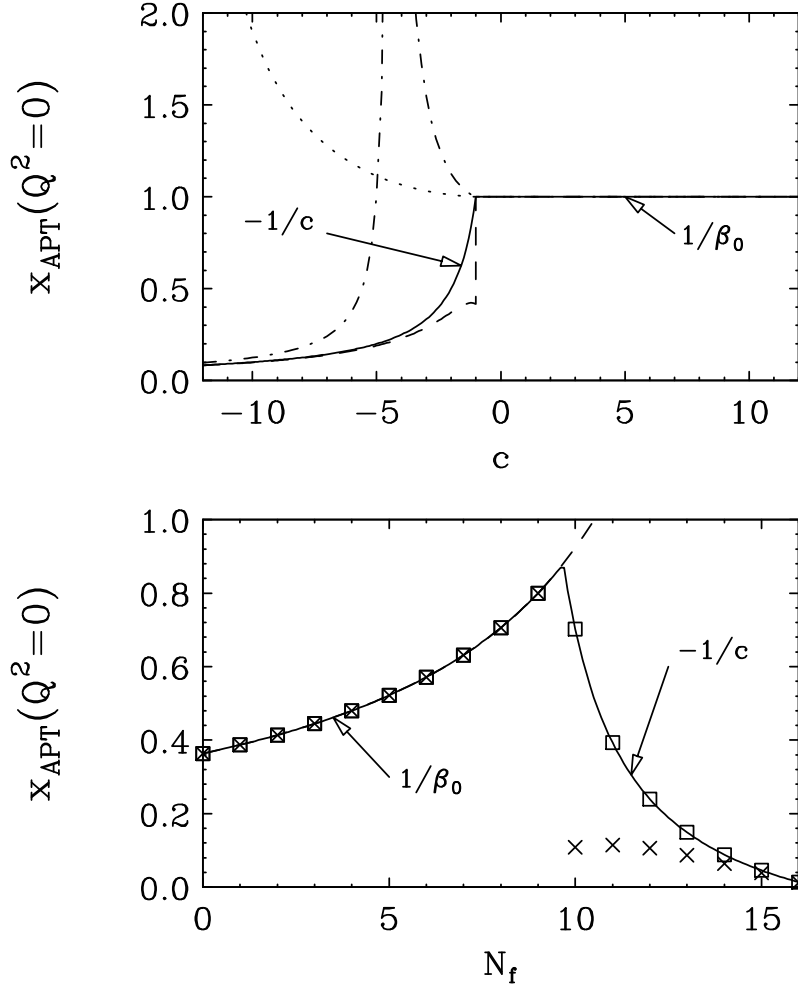


Figure 7: The upper box shows the infrared limit of the APT solution for a hypothetical PA-improved 3-loop  $\beta$  function with  $\beta_0 = 1$ , a span of values for  $c$ ,  $-12 < c < 12$  and various values for  $c_2$ . Continuous line:  $c_2 = 0$  (the 2-loop case), dashed line:  $c_2 = -1.4$ , dot-dashed line:  $c_2 = 20$ , dotted line:  $c_2 = 200$ . The lower box shows  $x_{\text{APT}}(0)$  in QCD with  $0 \leq N_f \leq 16$ . Squares and crosses correspond to a 2-loop and a PA-improved 3-loop  $\overline{\text{MS}}$   $\beta$  function, respectively. For  $N_f \leq 9$ ,  $x_{\text{APT}}(0)$  is  $1/\beta_0$  in both cases.